1340027

by Colombo Celso Gaeta Tassinari, Kátia Maria Mellito and Marly Babinski

Age and origin of the Cu (Au-Mo-Ag) Salobo 3A ore deposit, Carajás Mineral Province, Amazonian Craton, northern Brazil

Centro de Pesquisas Geocronógicas, Instituto de Geociências, Universidade de São Paulo, Rua do Lago 562, São Paulo, Brazil. CEP 05588-080, E-mail: ccgtassi@usp.br

The Salobo 3A polymetallic Cu (Au-Mo-Ag) deposit, located in the southeastern part of the Amazonian Craton, northern Brazil, is hosted by an Archean metavolcano-sedimentary sequence of Salobo Group. The copper mineralization consists of bornite-chalcocite and bornite-chalcopyrite disseminated with magnetite.

In this paper we attempt to date the mineralization episodes and to characterize the fluid sources. The stepwise Pb leaching technique applied to chalcocite, tourmaline, chalcopyrite and magnetite yielded ^{207}Pb-^{206}Pb ages of 2705 ± 42 Ma, 2587 ± 150 Ma, 2427 ± 130 Ma, and 2112 ± 12 Ma, respectively. The older age is interpreted as the timing of primary mineralization. Ages of 2.58 Ga and 2.42 Ga are considered to be related to tectonic reactivation of the Itacaiúnas Belt, and the younger age, obtained on late magnetite crystals, suggests the presence of Paleoproterozoic hydrothermal episode. Sm-Nd and Rb-Sr ages of 2.4 and 2.1 Ga were obtained for schists from the Salobo Group and chloritized gneisses of the Xingú Complex, respectively.

The strong radiogenic Pb isotopic compositions of all analyzed minerals suggest a continental environment for the mineralizations.

Our geochronological results are in agreement with a primary syngenetic origin for the Salobo mineralization, with late remobilization into brittle-ductile structures during a policyclic evolution of the Carajás-Cinzento strike-slip system. Low-grade metamorphism and anorogenic granitic plutonism affected the area at ca. 2.1 and 1.8 Ga, respectively.

Introduction

The Salobo 3A ore deposit is located in the southern part of the Amazonian Craton, within the Central Amazonian Province (Tassinari and Macambira, 1999) in the Serra dos Carajás area, and it is represented by an elongated mountain near the coordinates 5°32'S and 50°31'W. It constitutes part of the Carajás Mineral Province, which is the most important metallogenetic province of South American Platform. The reserves of the ores of the Salobo 3A polymetallic deposit are around 1.4 billion tonnes for copper with average grades of 0.8%, and 530 tonnes for gold with concentrations of 0.48 g/ton (Alves and Marques, 1994). This ore deposit was studied by several authors, like Farias and Sauressig (1982), Tassinari et al. (1982), Guimarães (1987), Lindenmayer (1990), Siqueira (1990), Machado et al. (1991), Lindenmayer et al. (1994), Réquia et al. (1997), Figueiredo et al. (1994), Siqueira (1996), and Pinheiro and Holdsworth (1997), with reference to their petrographic aspects, tectonic structures, geochronology, metamorphism and geological setting.

In this paper we attempt to (a) define the range of the Pb isotopic compositions of ore and gangue minerals from the Salobo 3A polymetalic deposit and use the Pb isotopic characteristics as constrains on mineralization modelling, (b) identify the nature of the sources, and (c) date the different mineralization episodes and superimposed metamorphic events using also Rb-Sr and Sm-Nd systematics. The isotopic analyses were undertaken in order to investigate the chronological evolution of the ores and their respective relationship with the regional geological history.

The dating of sulphides and gangue minerals by Pb-Pb leaching stepwise technique is potentially one of the most useful methods developed for directly dating Archean and Paleoproterozoic ore deposition (Bjorlykee et al. 1990, Frei and Kamber, 1995; Frei and Pettke, 1996).

Regional geologic setting

The Carajás area is part of the E-W trending Itacaiúnas Belt, which is bounded to the east by the Neoproterozoic Araguaia—Tocantins Belt, to the west by Mesoproterozoic volcanic and sedimentary covers, to the south by Archean granite-greenstone terrain, and Paleozoic to Cenozoic sediments of the Amazon Basin occur to the north (Figure 1).

According to Pinheiro and Holdsworth (1997), the stratigraphy of the Itacaiúnas Belt comprises an Archean basement assemblage, dominated by orthogneisses with granite-tonalitic composition named Pium Complex, syn-tectonic granitoids (Plaquê Suite), amphibolite, gneisses and migmatites (Xingú Complex) and an younger metavolcano-sedimentary sequence, affected by medium- to high-grade metamorphism, the so-called Salobo Group. The basement is unconformably overlain by a cover assemblage composed of low- to very low-grade volcanic and sedimentary rocks. This assemblage comprises the Igarapé Pojuca Group, Grão Pará Group and the Águas Claras Formation. The Estrela orthogneiss is intrusive into both the basement and Igarapé Pojuca Group. Paleoproterozoic intrusive anorogenic granitoids are widespread in the area. The sedimentary Gorotire Formation overlay all older lithological units.

The evolution of the Itacaiúnas Belt is complex and believed to have started shortly after the crystallization of the basement rocks in the region. A zircon U-Pb age of 2.86 Ga was determined for the

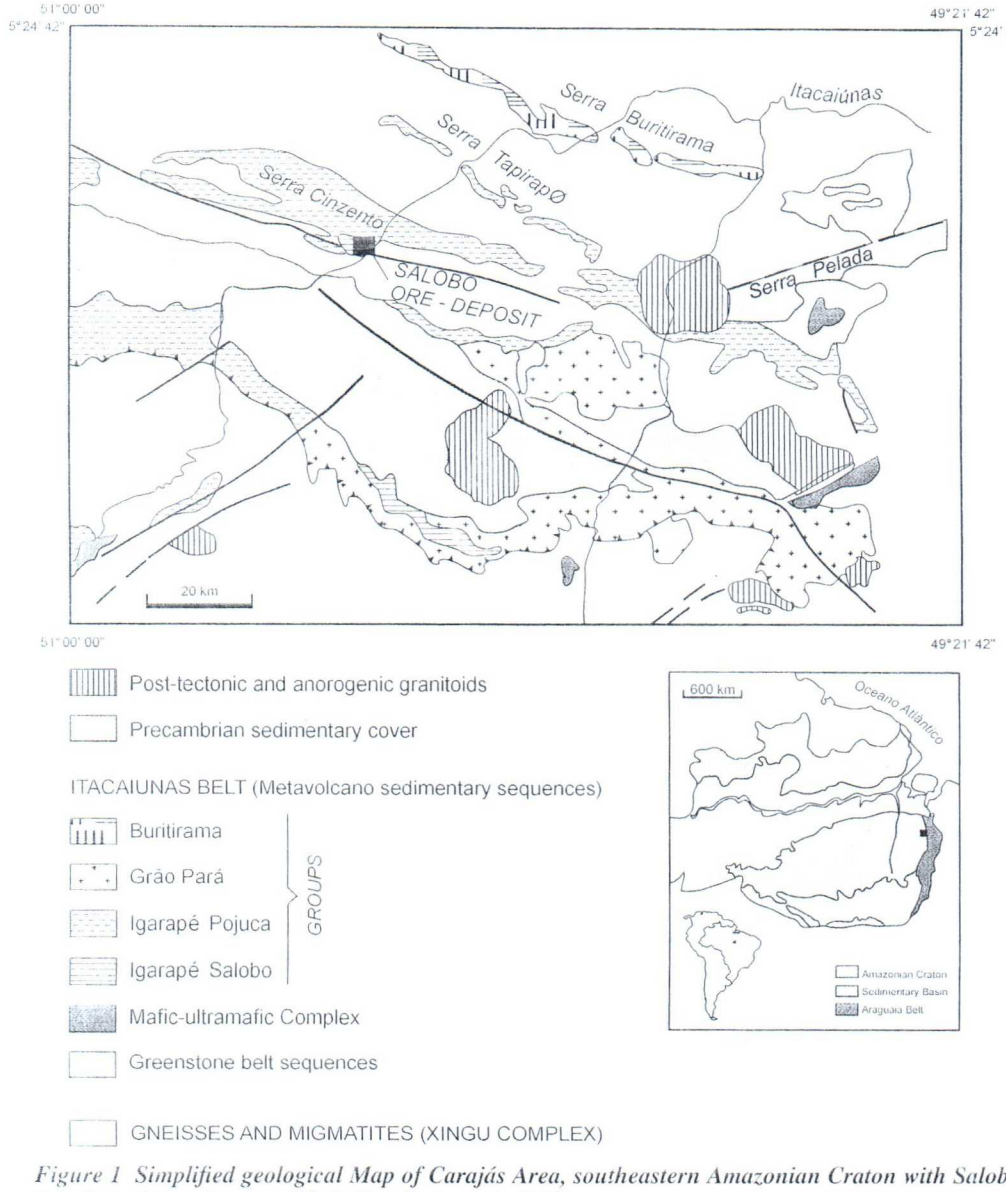

Figure 1 Simplified geological Map of Carajás Area, southeastern Amazonian Craton with Salobo Ore Deposit location (modified after Costa et al. 1995).

tonalitic gneisses, and is interpreted as a rock-formation age (Machado et al. 1991).

The development of transpressional deformational regime in the Itacaiúnas Belt, possibly, can be correlated with the deposition of the volcano-sedimentary sequence of the Pojuca and Grão ParáGroups in an extensional basin. The time of the beginning of sedimentation remains uncertain, nevertheless, a zircon U-Pb age of 2,761 ± 3 Ma from foliated amphibolite of the Salobo Group was interpreted as dating the amphibolite facies metamorphism in the area (Machado et al. 1991), suggesting an older age for the Salobo Group deposition. In addition, the zircon U-Pb age of 2,759 ± 2 Ma determined on metarhyolites and metarhyodacites of the Grão Pará Group was interpreted as the time of the bimodal volcanism (Machado et al. 1991). Subsequent movements resulted in the formation of the Carajás-Cinzento strike-slip system, the Carajás fault and the basin inversion (Pinheiro and Holdsworth, 1997). These events took place between 2.6 and 2.5 Ga, as observed on the Estrela gneiss (2,527 ± 34 Ma, whole-rock Rb-Sr isochron, Barros et al. 1992), on the gneisses of Xingú Complex and Rio Maria granitoid (2,480 ± 30 Ma and 2,660 ± 40 Ma, respectively, whole-rock Rb-Sr isochron, Montalvão et al. 1984). Those ages were interpreted as resetting ages of a low-grade metamorphic event. Moreover, a zircon U-Pb age of 2,573 ± 2 Ma obtained on the Old Salobo Granite was interpreted as a rock-formation age (Machado et al. 1991).

The younger important event in the Carajás Mineral Province was the intrusion of several anorogenic granitoids between 1.92 and 1.88 Ga (Macambira and Lafon, 1995).

The geological evolution of the Carajás area, close the Salobo Ore Deposit, can be summarized as follows:

3.1–2.9 Ga—Rock-formation of the Tonalitic-Gneisses of Xingú Complex from mantle-derived material;

2.85–2.7 Ga—Volcanism and deposition of the metavolcano-sedimentary sequences of Salobo Group, followed by high- to medium-grade metamorphic events;

2.6–2.5 Ga—Tectonic reactivation process related to Carajás-Cinzento Shear Zone, together with emplacement of the granitic intrusions, like Old Salobo Granitoid;

1.92 and 1.88 Ga—Emplacement of anorogenic granitoids.

Salobo 3A ore deposit

The mineralization is hosted by a metavolcano-sedimentary sequence called Salobo Group. It is composed, from base to top, of lenses of iron formation, amphibolites, pelitic metassediments and quartzites. Its thickness varies between 300 and 600 m. A sequence of weathered rocks with thickness between 30 and 100 m covers the deposit (Figure 2).

The Salobo Group is cut by the 2.57 Ga I-type Old Salobo Granite, by 1.92–1.88 Ga anorogenic Young Salobo Granite and by Neoproterozoic diabase dykes related to NE-SW and NW-SE faults, as reported by Pinheiro and Holdsworth, (1997).

Both the metavolcano-sedimentary sequence and the Old Salobo Granite show a strong foliation. The sequences follow a general WNW-ESSE trend which is defined by a straight lineament developed under ductile conditions to the south of the deposit. Lineaments follow NW-SE, NNE-SSW and NE-SW directions, which converge in a curved structure to the north of the deposit (Pinheiro and Holdsworth, 1997). Those lineaments together constitute a sidewall ripout structure (Pinheiro and Holdsworth, 1997) or the Salobo-Mirim duplex (Siqueira, 1990).

Requia et al. (1997) reported two metamorphic events on the Salobo 3A deposit. The first one was associated with progressive amphibolite facies metamorphism developed under ductile conditions of high temperature (650°C), low pressure (2 to 3 kbar) and fO_2 between –20 and –18. The second one was retrograde and developed under greenschist facies, with an average temperature of 340°C, producing chloritization as hydrothermal alteration.

The copper mineralization is hosted by iron formation and it consists of bornite-chalcocite and bornite-chalcopyrite disseminations in magnetite rich zones. The ore occurs in pressure shadows of the minerals, fills microfractures of olivine, magnetite, garnet or encloses them, fills fractures of the iron formations, quartzites and

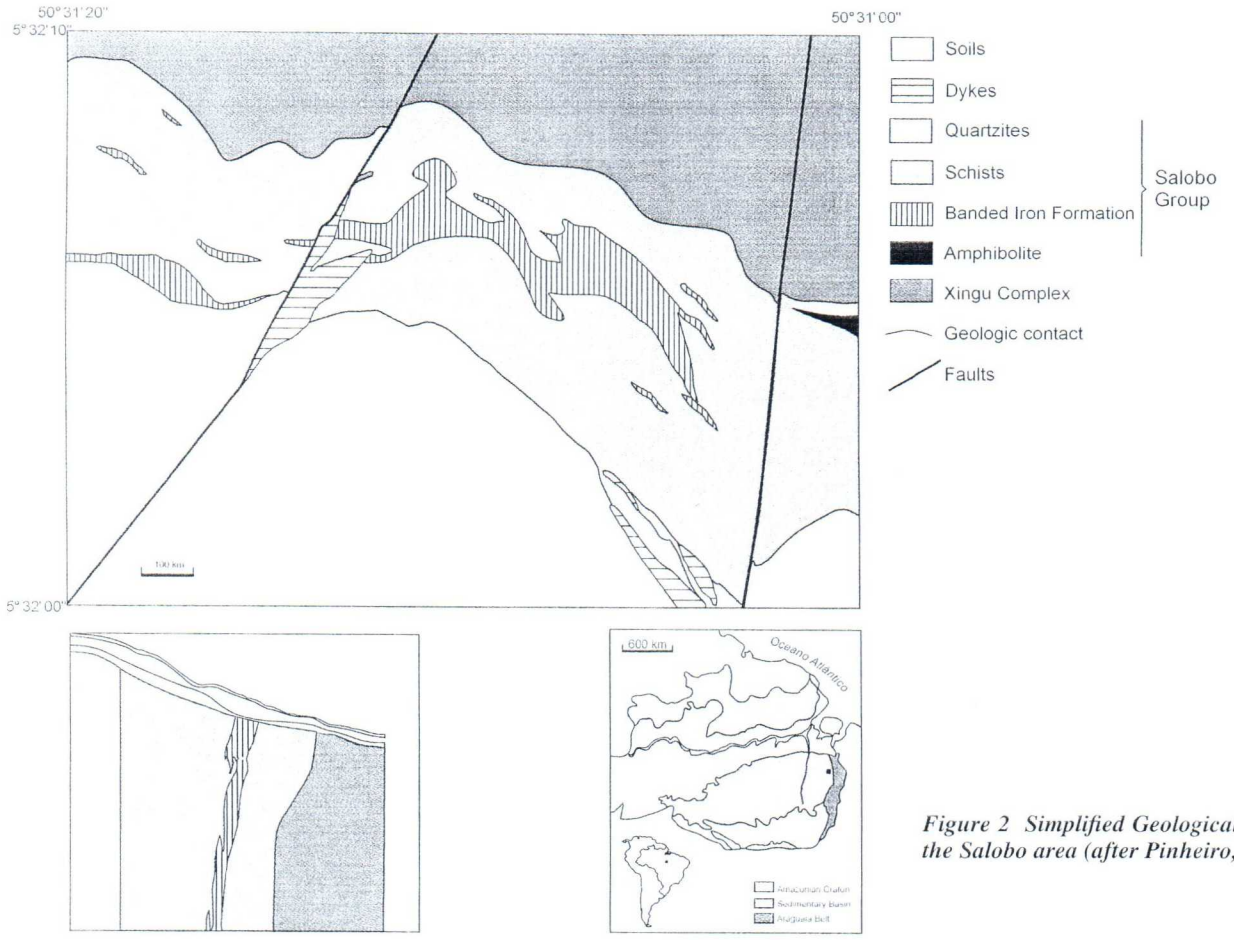

Figure 2 Simplified Geological Map of the Salobo area (after Pinheiro, 1997).

schists, and exists as inclusions as well. The tectonometamorphic processes were responsible for the copper redistribution into brittle structures. The copper content is > 0.8% in magnetite-schist and iron formation, while in gneisses and schists it is < 0.8%. Moreover, there is a positive correlation between the copper and uranium contents in this deposit (Nuclebrás, 1985).

Different kinds of genetic models have been discussed in the literature to explain the genesis of the Cu-Au Salobo Ore Deposit. Lindenmayer et al. (1994) proposed a mixing origin to the ores, including a volcanogenic exhalative source to the primary Cu mineralization and epigenetic genesis, related to 1.9 Ga Young Salobo Intrusion for the Au and Mo mineralization. Réquia et al. (1997) considered the Salobo mineralization related either to hydrothermal metamorphic fluids or to the 2.5 Ga Old Salobo granitic intrusion. Lindenmayer (1999) proposed a porphyry copper model for the ore deposit. Hunh and Nascimento (1997) admitted for all Cu-Au ore deposits of the Carajás area an origin similar to that of the Fe-Cu-Au-U-ETR model of Hitzman et al. (1992), where the ore fluids are derived from Archean granitoids.

Sampling

All analyzed samples were collected from drillholes.

The iron formation of sample F143/542.89m from the Salobo Group is composed of recrystallized quartz and magnetite, associated with bornite and chalcocite, and it is cut by sulphide (chalcopyrite) veins. The brecciated iron formation of sample F50/90.10m comes from the same unit and is composed of quartz and magnetite with bornite, chalcocite, gold and hydrothermal alteration minerals as accessories. In general magnetite is granoblastic, although in polished section it also appears in a continuous mass in which it is difficult to distinguish individual crystals.

The tourmaline quartzites of samples F143/450.0m and F143/278.8m belong to the quartzitic unit of the Salobo Group. The tourmaline does not have stretched feature, as observed on quartz, and it is typically euhedral with regular edges; commonly has optical zoning characterized by lighter cores enriched in Mg, and darker rims richer in iron. The sample F154/58.47m represents a tourmaline vein which cuts the tonalitic gneiss of the Xingú Complex.

The tonalitic gneisses samples (F12/493.3m, F24/251.4m, F19/259.06m, F147/32.7 and F147/59.75m) are from the XingúComplex. All samples occurs within the mineralized area and they are affected by hydrothermal alteration. They have a penetrative foliation and consist of chlorite, plagioclase, quartz, biotite, magnetite, bornite and opaques. Tourmaline occurs in metasomatized zones. Plagioclase is partially or totally replaced by chlorite and sericite depending on the intensity of the chloritization and/or sericitization. Biotite also is almost always replaced by chlorite, which characterize the sample as hydrothermal altered one.

The schist samples (F23/310.6m and F59/204.35m) belong to the Salobo Group, which is the host of the Cu(Au-Mo-Ag) mineralization. The first one is a garnet-quartz-grunerite schist, and the second sample is a biotite-quartz-garnet schist.

Analytical techniques

A total of 53 isotopic analyses on tourmaline, chalcocite, chalcopyrite, magnetite, calcites, brecciated iron formation, chloritized tonalitic gneisses, and schists were carried out at the Geochronological Research Center (CPGeo) of the University of São Paulo. The samples were cut and prepared for petrographic analyses and were described in terms of rock type, texture, mineral association, occurrence, and mineralization style.

The samples for whole-rock analysis were crushed and powdered in a ball-mill, while the samples for mineral isotopic analyses were sieved to grain size between 80 and 200 mesh. Mineral separation was done with eletromagnetic separator, hand-picked under a binocular microscope, and the unaltered grains were selected. The minerals ca. 500 to 600 mg of chalcocite, chalcopyrite, tourmaline and magnetite, and ca. 50 mg of calcite, amphibole and garnet were ultrasonically washed in triple distilled water, before the chemical attack.

For the Pb isotopic analyses a series of leaching treatments was carried out for tourmaline, chalcopyrite, magnetite and chalcocite, using a technique which was slightly modified after Frei and Kamber (1995) and Bjorlykee et al. (1990). After each step of leaching, the solute was recovered and the residue was washed 3 times with triple distilled water. The solutes were evaporated to dryness, converted to chloride form with 1 ml of 6N HCl and Pb was separated by the conventional HCl-HBr anion exchange technique. Pb separated were loaded on Re filaments together with 4µl of silica gel and phosphoric acid and analyzed statically by a VG 354 multicollector mass spectrometer.

A bulk sample of brecciated iron formation was totally dissolved with a mixture of HF and HNO_3 in a proportion of 2:1, then converted to chloride form. Total procedural blanks were 210 pg for both tourmaline and sulfides and 400 pg for magnetite and iron formation whole-rock. Isotopic values were corrected for mass fractionation of 0.12% a.m.u^{-1}, using multiple analyses of Common Pb NBS 981 standard. Isochron ages were calculated using ISOPLOT program of Ludwig (1998). The age errors are quoted at 95% confidential level.

Rb-Sr isotopic analysis followed the standard procedures of the CPGeo laboratory. The whole-rock gneisses and tourmalines samples were totally digested with HF plus HNO_3 in a proportion of 2:1. The solutions were evaporated to dryness; converted to chloride form with 2.62N HCl and Sr was separated in AG 50W-X8, 200-400 mesh cationic resin. The Sr samples were loaded on Ta filaments together with 2µl H_3PO_4 and analyzed in the 354 VG mass spectrometer. The Rb concentrations were measured by X-ray fluorescence technique. The reproducibility was controlled by the NBS 987 standard analyses, averaging a value of $^{87}Sr/^{86}Sr = 0.71024 \pm 0.00002$. Total procedure blank for Sr was 5 ng. The age was calculated using ISOPLOT program of Ludwig (1998).

Sr isotopic analyses were performed on calcite. The calcite was totally dissolved with 0.1N HCl: the solutes were evaporated to dryness and converted to chloride form by 2.62N HCl; Sr was separated on ion exchange columns in the same way as described above.

Samples for Sm-Nd analyses were dissolved using the same procedure described for Rb-Sr analyses, after adding ^{150}Nd-^{149}Sm spike. The solutes were evaporated, converted with 0.2 ml 2.5N HCl and the rare earth elements (REE) were separated with 6.2N HCl in a AG 50W-X8, 200-400 mesh cationic exchange resin. Afterwards, the solutions were dried and diluted with 0.26N HCl and loaded through ion exchange columns. Sm and Nd were eluted with 0.26N HCl and 0.55N HCl. Both elements were loaded as phosphates on Re filaments. Measurements of $^{143}Nd/^{144}Nd$ were normalized to $^{146}Nd/^{144}Nd = 0.719$. Repetitive analysis of the La Jolla standard was used to calculate reproducibility. The isochron ages were calculated using ISOPLOT software of Ludwig (1998).

Results and discussion

Pb isotopic analyses were carried out on chalcocites, chalcopyrites, tourmalines and magnetites using the stepwise leaching technique.

Leachate and residue data obtained on chalcocites presented very radiogenic Pb isotopic ratios with $^{206}Pb/^{204}Pb$ values between 274.6 and 366.4, $^{207}Pb/^{204}Pb$ from 62.82 to 80.08, and $^{208}Pb/^{204}Pb$ from 87.9 to 107.5, as reported in Table 1. All measured isotopic ratios are strongly radiogenic, possibly due to the high content of U and Th in the mineralizing fluid and/or the presence of U and Th-bearing minerals as solid inclusion in the chalcocite. In this way, an internal report of Nuclebrás (1985) showed anomalous U_3O_8 and ThO_2 concentrations in the host iron formation, which could be the U and Th-enriched source.

If all analytical points are plotted in the $^{207}Pb/^{204}Pb$ vs. $^{206}Pb/^{204}Pb$ diagram, they show some dispersion, and the points are located around the line with a slope that corresponds to an age of 2,762 ± 180 Ma. The scattering of some analytical points reflects post-mineralization disturbance produced by superimposed brittle tectonic reactivation, which could produce a mixing of ore fluids, considering that the sulfides have relatively high solubility in intergranular water.

Nevertheless, taking into account the leachates L1, L3, L4 and the residue for the chalcocite, it is possible to calculate a Pb-Pb isochron age of 2,705 ± 42 Ma (Figure 3), which could be interpreted

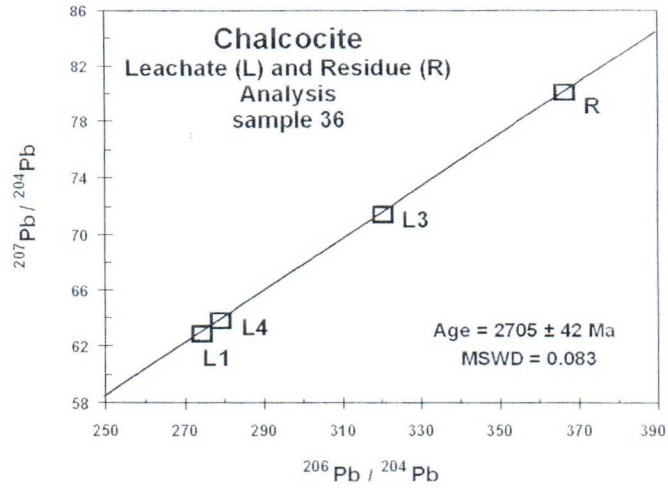

Figure 3 Pb-Pb isochron diagram for chalcocite (leachates + residue) from Salobo Deposit.

as the age of the primary mineralization, reflecting the approximate timing of the syngenetic episode. This age is compatible with the Pb-Pb age of 2764 ± 22 Ma obtained on chalcopyrite and gold from the Igarapè Bahia gold deposit (Galarza 2002). Late Archean Pb-Pb ages interpreted as the time of the primary Cu, Au and U mineralization (Mougeout et al., 1996), were also determined on sulfide minerals of the Igarapé Pojuca Group.

The Pb stepwise leaching technique was also applied to secondary (remobilized) chalcopyrite, which occurs mainly filling microfractures. The chalcopyrite and their leachates yielded radiogenic Pb isotopic compositions with $^{206}Pb/^{204}Pb$ varying from 231.4 to 246.7, $^{207}Pb/^{204}Pb$ from 65.42 to 67.66, and $^{208}Pb/^{204}Pb$ from 49.7 to 50.8 (Table 1). Three of the five analyzed products (the leachates 1 and 3 and the residue) defined a line with a slope corresponding to a Pb-Pb age of 2,427 ± 130 Ma (Figure 4). Despite of the high error, the age could be related to the time of the Carajás - Cinzento Shear Zone, which would be responsible for the sulfide remobilization episode.

Tourmaline samples belonging to the tourmaline-quartzite of the Salobo Group and to vein-type tourmaline which occurs cross-cutting the gneisses of the Xingú Complex were also analyzed. Leachates from tourmaline yielded highly radiogenic Pb isotopic compositions with $^{206}Pb/^{204}Pb$ ranging from 1,409 to 224.5, $^{207}Pb/^{204}Pb$ from 224.37 to 37.76 and $^{208}Pb/^{204}Pb$ from 3,110 to 139.3. According to Nuclebrás (1985) there is a positive correlation between the MgO and U_3O_8 content in schists, quartzites and gneisses around the Salobo 3A Deposit. As the tourmalines belong to the schorlite-dravite series, and most of them have a Mg-bearing core, this could explain the very high Pb isotopic compositions in this mineral. In the $^{207}Pb/^{204}Pb$ vs. $^{206}Pb/^{204}Pb$ diagram (Figure 5) the leachates and the residue from the two types of tourmalines were plotted together. The analytical data which presented evidence of isotopic disequilibrium were omitted, and the calculated age, using

Table 1 Pb isotopic data determined by stepwise leaching technique.

Leachate	Material	$^{206}Pb/^{204}Pb$	$^{207}Pb/^{204}Pb$	$^{208}Pb/^{204}Pb$
Sample F143/542.89 (Alterated Iron Formation)				
L1	Chalcocite	274.552 (0.13)	62.867 (0.13)	87.851 (0.13)
L2		347.969 (0.66)	77.705 (0.56)	104.504 (0.54)
L3		320.603 (0.30)	71.392 (0.30)	97.651 (0.30)
L4		279.268 (0.28)	63.757 (0.28)	89.118 (0.28)
R		366.639 (0.90)	80.085 (0.90)	107.477 (0.90)
SampleF46/417.10 (Iron Formation)				
L1	Chalcopyrite	231.440 (0.03)	65.417 (0.02)	50.763 (0.03)
L2		240.807 (0.26)	66.122 (0.26)	49.669 (0.26)
L3		246.668 (0.42)	67.655 (0.42	50.511 (0.42)
L4		239.235 (0.14)	66.346 (0.14)	50.344 (0.14)
R		236.048 (0.08)	66.162 (0.08)	50.611 (0.08)
Sample F154/58.47 (Vein-type Tourmaline)				
L1	Turmaline	694.395 (0.48)	105.839 (0.48)	3109.789 (0.48)
L2		901.390 (1.25)	134.701 (1.25)	2788.332(1.25)
L3		550.030 (0.74)	93.500 (0.74)	1113.926(0.74)
L4		719.886 (0.55)	123.169 (0.55)	892.987(0.55)
R		619.214 (3.74)	110.482 (3.72)	372.289(3.76)
Sample F143/250.0 (Tourmaline Quartzite)				
L1	Turmaline	537.007 (0.06)	94.308 (0.06)	169.470 (0.06)
L3		1408.977 (1.30)	224.376 (1.30)	89.875 (1.30)
L4		1135.970 (0.50)	183.814 (0.50)	94.840 (0.50)
R		714.511 (0.64)	147.632 (0.63)	238.731 (0.63)
Sample F143/278.8 (Tourmaline Quartzite)				
L1	Turmaline	484.94 (0.12)	88.188 (0.07)	248.262 (0.07)
L2		617.616 (0.28)	106.792 (0.28)	745.442 (0.28)
L3		320.069 (0.76)	57.017 (0.76)	139.272 (0.76)
L4		224.541 (0.80)	37.764 (0.80)	133.377 (0.80)
R		522.150 (5.60)	136.472 (5.40)	196.932 (5.40)
Sample F50/90.10 (Banded Iron Formation)				
L1	Magnetite	135.879 (0.19)	31.094 (0.19)	79.965 (0.19)
L2		223.028 (0.09)	42.665 (0.09)	105.405 (0.11)
L3		29.401 (0.04)	17.641 (0.04)	42.231 (0.04)
L4		81.699 (0.07)	26.993 (0.06)	61.500 (0.06)
L5		22.528 (0.27)	16.442 (0.21)	38.959 (0.32)
L6		29.864 (1.00)	17.469 (1.00)	40.918 (1.40)
R		87.516 (0.11)	29.466 (0.12)	60.393 (0.11)
T	WR	138.706 (0.22)	33.939 (0.22)	74.982 (0.22)
40	BIF	163.791 (0.09)	36.843 (0.09)	89.275 (0.09)

Notes: All the isotopic ratios were corrected for mass fractionation. Numbers in parenthesis represent 1-sigma errors (%); L =Leachates; R = residue; T = total dissolution; WR = whole-rock.

four leachates and the residue was 2,587 ± 150 Ma. Considering the analytical error, the age obtained for the tourmalines is in agreement with the chalcopyrite Pb-Pb age. Furthermore, these ages can be correlated with a regional reactivation period, which promoted the development of the Carajás—Cinzento strike-Slip System (2,573 — 2,479 Ma; Pinheiro and Holdsworth, 1997). The same age interval was detected by the Rb-Sr age of 2,497 ± 62 Ma determined on metarhyolites from Pojuca Group (Olszewski et al., 1989). This event could have produced a fluid flow and subsequent formation of tourmalines in the quartzites.

Leachate-residue and bulk analyses of euhedral younger magnetite (Table 1) and the brecciated iron formation whole rock also yielded very radiogenic Pb isotopic compositions and the release pattern of Pb was not systematic. $^{206}Pb/^{204}Pb$ range from 22.52 to 223.0, $^{207}Pb/^{204}Pb$ from 16.44 to 42.67 and $^{208}Pb/^{204}Pb$ from 40.9 to 105.4. In the $^{207}Pb/^{204}Pb$ vs. $^{206}Pb/^{204}Pb$ diagram (Figure 6) the data do not define a linear array due to the presence of uraninite inclusions in the magnetite (Réquia et al., 1997), which could produce Pb isotopic evolution with different μ values for several analyzed

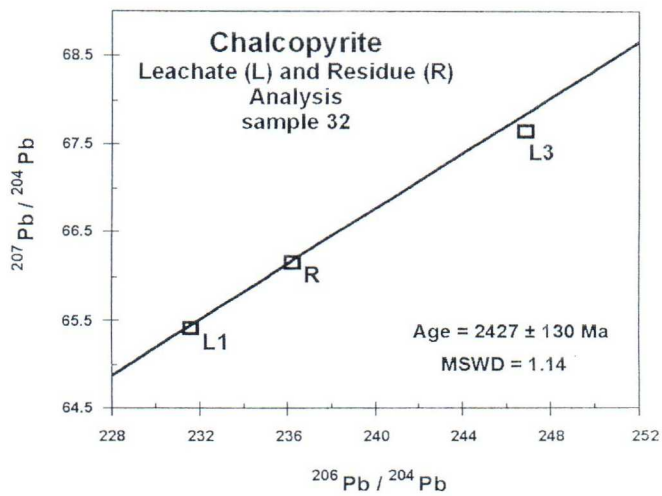

Figure 4 Pb-Pb isochron diagram for chalcopyrite (leachates + residue) from Salobo Deposit.

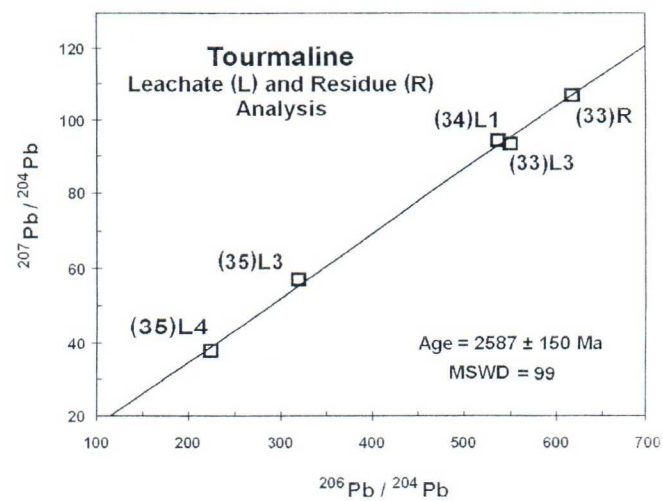

Figure 5 Pb-Pb isochron diagram for tourmaline (leachates + residue) from Salobo Deposit.

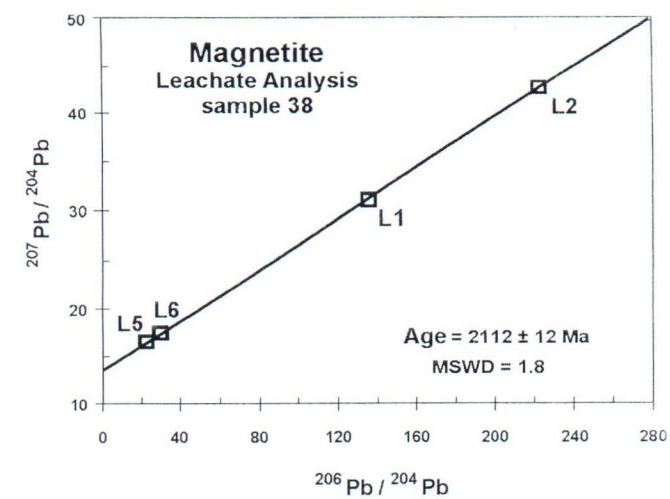

Figure 6 Pb-Pb isochron diagram for magnetite (leachates) from Salobo Deposit.

leachates. Nevertheless the leachates 1, 2, 5 and 6 define an isochron age of 2112 ± 12 Ma. This age suggests a close relationship between the later magnetite formation and the Paleoproterozoic Transamazonic event.

According to Réquia et al. (1997) the banded iron formations were affected by K-hydrothermal alteration (650–550°C) followed by a strong propylitization event (350–270°C), characterized by the development of chlorites. In order to confirm these hypothesis, whole-rock Rb-Sr analyses were performed on seven hydrothermal altered tonalitic gneisses affected by this propylitization event. The analytical results are reported in Table 2, and plotted in a Rb-Sr isochron diagram (Figure 7). The data defined an errorchron with a slope corresponding to an age of 2,101 ± 130 Ma, with an initial $^{87}Sr/^{86}Sr$ ratio of 0.7281 ± 0.0043. Despite the possible partial isotopic disequilibrium, this age is interpreted as dating the chloritization process, showing a chronocorrelation between this hydrothermal event and the later magnetite formation. In addition, these ages are compatible with other Paleoproterozoic ages like that of 2,029 ± 21 Ma (Rb-Sr whole-rock, Gomes et al., 1975) and 1,987 ± 77 Ma (K-Ar on amphiboles, Gomes et al., 1975) determined on gneisses from the northeast of the Salobo Deposit area.

One garnet-quartz-grunerite schist and one biotite-quartz-garnet schist from the Salobo Group were chosen for Sm-Nd isotope analyses on mineral separates. The geochronological data are in Table 3 and plotted in Figure 8. The analytical data defines a mineral isochron age of 2,430 ± 37 Ma, with a $(^{143}Nd/^{144}Nd)i$ of 0.509346 ±0.000085 (MSWD = 4.4) and ε_{Nd} value of —2.7, calculated for 2.4 Ga. As the schist samples present evidence of retrometamorphism on biotite and garnet, involving temperature around 350°C associated with metamorphic fluid flows, it is probable that the garnet geochronometer was reset during this event, at ca. 2.4 Ga, at the same period of the chalcopyrite and tourmaline remobilizations.

Nine $^{87}Sr/^{86}Sr$ analyses were performed on calcites and tourmalines to define the possible fluid sources. Results are reported in Table 2.

Because calcites have negligible Rb contents and high Sr contents, their $^{87}Sr/^{86}Sr$ isotopic compositions may reflect the Sr isotopic ratio of fluid from which the mineralization was formed. The total range of $^{87}Sr/^{86}Sr$ ratios for calcites, which occur as hydrothermal alteration products, associated with iron formations and amphibole schists of Salobo Group, is from 0.73924 to 0.75757. The very radiogenic Sr isotopic compositions are typical for Sr with a prolonged crustal history before fluid interaction and/or for Sr introduced by hydrothermal fluids mixed with the Sr released during fluid

Table 2 Rb - Sr analytical data.

Sample	Host-Rock	Rock type	Rb (ppm)	Sr (ppm)	$^{87}Rb/^{86}Sr$	Error	$(^{87}Sr/^{86}Sr)^*$	Error	$(^{87}Sr/^{86}Sr)^{**}$
F142/58.57		Gneiss	10.0	43.2	0.673	0.006	0.74792	0.00010	
F147/32.7		Gneiss	39.9	26.7	4.385	0.037	0.85995	0.00009	
F12/493.3		Gneiss	17.5	81.4	0.624	0.069	0.74353	0.00006	
F19/259.06		Gneiss	54.0	163.8	0.958	0.009	0.75940	0.00008	
F19/258.0		Gneiss	79.9	102.1	2.286	0.064	0.79791	0.00080	
F24/251.4		Gneiss	81.1	130.2	1.817	0.051	0.78467	0.00010	
F147/59.75		Gneiss	72.3	29.3	7.344	0.061	0.97358	0.00009	
F66/422.3	FF	Calcite	ND	113.5			0.74126	0.00006	
F154/4666.54	FF	Calcite	ND	132.4			0.73924	0.00006	
F41/327.7	FF	Calcite	2.4	100.2			0.74631	0.00010	
F147/260.68	A-Schist	Calcite	ND	50.0			0.75757	0.00010	
F143/245.25	Vein-T	Tour.	18.0	34.9			0.77197	0.00008	0.73963
F154/58.47	Vein-T	Tour.	19.4	69.3			0.77717	0.00007	0.75961
F143/250.0	T-qz	Tour.	0.5	56.2			0.71696	0.00008	0.71641
F142/233.45	T-qz	Tour.	6.2	84.6			0.72449	0.00008	0.71992
F143/278.8	T-qz	Tour.	2.9	75.2			0.71499	0.00008	0.71209

Notes: FF = Iron Formation; Vein-T = Tourmalinites (veins); T-qz = Tourmaline quartzite; Tour = tourmaline. A-Schist = Amphibole-Schist; ND = Concentrations below the detection limit (< 0.1 ppm). Errors are 1-sigma. * measured isotopic ratios. ** Isotopic ratios calculated back to 2.5 Ga.

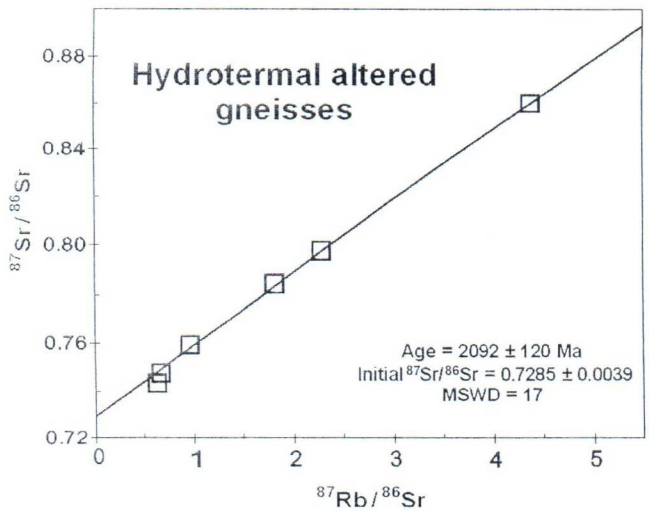

Figure 7 Rb-Sr isochron diagram for hydrothermal altered gneiss of Xingu Complex.

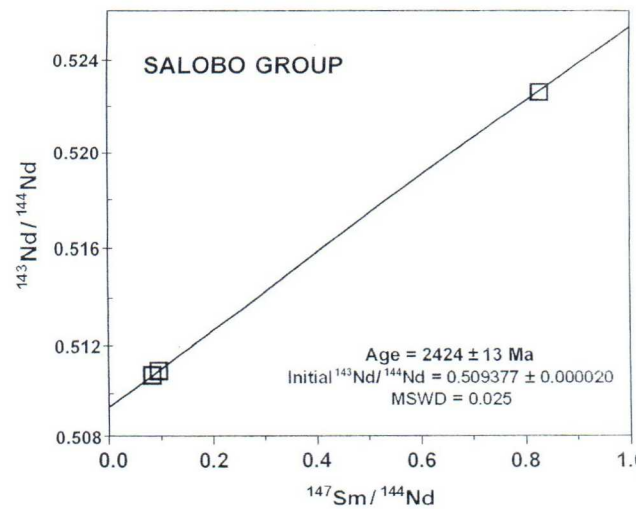

Figure 8 Sm-Nd isochron diagram for schist of Salobo Group.

Table 3 Sm-Nd analytical data from schists of the Salobo Group.

Sample	Material	Sm (ppm)	Nd (ppm)	$^{147}Sm/^{144}Nd$	Error	$^{143}Nd/^{144}Nd$	Error
Garnet-quartz-grunerite schist							
F23/310.6	WR	14.43	90.22	0.097290	0.000560	0.510931	0.000019
F23/310.6	grunerite	8.291	48.76	0.103474	0.000060	0.511004	0.000026
F23/310.6	garnet	2.398	1.748	0.829660	0.002843	0.522636	0.000041
Biotite-quartz-garnet schist							
F59/204.35	WR	6.099	43.61	0.085099	0.000047	0.510739	0.000029
F59/204.35	biotite	0.205	1.387	0.090056	0.000103	0.510713	0.000058

Notes: WR = whole-rock; Errors are 1-sigma.

interaction with the host rocks. In this way, it is important to observe that the highest $^{87}Sr/^{86}Sr$ ratio (0.75757) was measured in hydrothermal calcite from the amphibole-schist, which is radiogenic Sr-enriched.

The initial $^{87}Sr/^{86}Sr$ ratios of the tourmalines, calculated for an estimated age of 2.5 Ga showed much larger variation (0.71209 to 0.75961). The tourmalines from the quartzites have less radiogenic Sr isotopic compositions (0.71209 to 0.71992) compared to the tourmalines from the tourmalinites and to the gneissic complex rocks (0.73963 to 0.75961). Considering the Sr isotopic compositions from the calcites and tourmalines, it is reasonable to assume that the fluids evolved within continental environment.

Final consideration

The multi-isotopic systems applied to minerals from different paragenetic sequences of mineralization and host-rocks of the Salobo 3A ore deposit revealed a geologically complex metallogenetic model, which developed as the result of, at least, three-stage, beginning with volcanism and deposition of the Salobo Group at ca. 2.7 Ga. Some re-equilibration and ore remobilization occurred around 2.5 Ga, related to the development of the Carajás-Cinzento strike-slip system and the later stage, took place at ca. 2.1 Ga, which is associated with retrograde greenschist facies metamorphic episode, with an average temperature of 340°C producing chloritization as hydrothermal alteration.

The geodynamic setting, in which the Carajás Basin developed, was interpreted as an extensional continental rift by Lindenmayer (1990) and Pinheiro (1997) or described as a pull apart basin by Siqueira (1990), Araújo and Maia (1991) and Costa et al. (1994). Afterwards, the Carajás basin suffered tectonic reactivations with the Carajás-Cinzento strike-slip development followed by basin inversion and formation of the pull apart basin. Those events could be related to the reworking and reprecipitation of sulfides into fractured zones. During the Paleoproterozoic low-grade retrometamorphism caused the precipitation of the younger magnetite, and the hydrothermal alteration of the older rocks as well.

The Pb and Sr isotopic compositions determined on the gangue and on the ore minerals provide geochemical evidence for a continental crust environment as source for some metals in the Salobo ore deposit.

Based on available geochronological data and on our new isotopic results the geological evolution of the area of the Salobo 3A deposit can be summarized as follows:

Ca. 3,000 Ma Mantle-crust differentiation and crystallization of the tonalite-gneissic basement (Xingú Complex)

2,850 — 2,750 Ma Volcanism and deposition of the Salobo, Pojuca and Grão Pará Groups in a continental setting. Development of the primary copper mineralization, mainly syngenetic, with U and Th-bearing fluids associated.

Ca. 2,500 Ma Tectonic reactivation processes with development of the Carajás-Cinzento strike-slip system and Old Salobo Granite intrusion. Metasomatic activities with boron, U and Th-rich fluids, tourmaline crystallization and chalcopyrite and molybdenite reprecipitation (epigenetic mineralization).

Ca. 2,100 Ma Hydrothermal alteration associated with low-grade metamorphism which promoted the magnetite precipitation.

1,920–1,880 Ma Anorogenic granitic activities.

In conclusion, our isotopic results are in accordance with a syngenetic model for the deposition of the primary cooper mineralization, with subsequent mobilization and reprecipitation of ore minerals (chalcopyrite and molybdenite) along shear zones, together with some possible magmatic activity during this time until at least 2,450 Ma ago. Later magnetite grains are related to the 2.1 Ga chloritization hydrothermal event. The very radiogenic Pb isotopic compositions of all analyzed minerals support the genetic models invoking hydrothermal activities percolating U-Th-enriched continental rocks.

Acknowledgements

We thank to the organizers of the field work to Carajás area, Vitório *Takai (in memorial)*, Nelson Barquesar, Vicente Fortes, Jose Alves Santos Filho of the Salobo Metais Ltda, Eduardo Angelim of the DOCEGEO, Bernardino Figueiredo and Roberto Perez Xavier of the University of Campinas. The staff of the CPGeo Liliane Petronilho, Arthur T. Onoe, Ivone K. Sonoki, and Helen M. Sonoki are thanked for their helpful technical support. We are grateful for the comments and criticisms of Jorge Bettencourt, João B. Moreschi, Gergely Szabó and Robert Frei. We thank also to FAPESP (Project 95/4652-2) and MCT (PRONEX 167/96), for the financial support to carry out this investigation. CCGT and MB thank CNPq for the Research Fellowships.

References

Almaraz, J. S. V., 1967, Determinações K-Ar na região do curso médio do Tocantins: Boletim da Sociedade Brasileira de Geologia, v. 16, no. 1, pp. 121-126.

Alves, F., and Marques M., 1994, Cobre Salobo. O maior projeto de mineração da década: Brasil Mineral, v. 122, pp.12-17.

Araújo, O. J. B., and Maia, R. G. N., 1991, Programa de levantamentos geológicos básicos do Brasil. Folha SB 22-Z-A. Serra dos Carajás, Estado do Pará. Projeto Especial Mapas de Recursos Minerais de Solo e de Vegetação para a área do Projeto Grande Carajás: Subprojeto Recursos Minerais. CPRM. Brasília. 164pp. 2 maps.

Barros, C. E. M., Dall'Agnoll, R., Lafon, J. M., Teixeira, N. P., and Ribeiro, J. W.,1992, Geologia e geocronologia do gnaisse Estrela, Curinópolis, PA: Boletim do Museo Paraense Emílio Goeldi, Série Ciências da Terra, v. 4, pp. 85-104.

Bjorlykke, A., Cumming, G., L., and Krstic, D., 1990, New isotope data from davidites and sulphides in the Bidjovagge gold-copper deposit, Finnmark, Northern Norway: Mineralogy and Petrology, v .43, pp. 1-21.

Costa. J. B. S., Araújo, O. J. B., Jorge João, X. S., Maia, R. G. N., Macambira, E. M. B., Vale, A. G., Santos, A., Pena Filho, J. I., and Neves, A. P., 1994, Panorama tectono-estrutural da Região Sudeste do Pará: 4th Amazonian Geological Symposium, pp. 314-317.

Farias, N. F., and Saueressig, R., 1982, Salobo 3A copper deposit: Int. Symp. Archean. Early Proterozoic Geol. Evol. & Metal. Excursion guide. Salvador, pp. 67-76.

Figueiredo, B. R., Réquia, K. C. M., and Xavier, R. P., 1994, Post depositional changes of the Salobo ore deposit, Carajás Mineral Province, Northern Brazil: Comunicaciones, University of Chile, v. 45, pp. 23-32.

Frei, R., and Kamber, B. S., 1995, Single mineral lead-lead dating: Earth Planetary Science Letters, v. 129, pp. 261-268.

Frei, R., and Pettke, T., 1996, Mono-sample Pb-Pb dating of pirrhrotite and tourmaline: Proterozoic vs. Archean intracratonic gold.mineralization in Zimbabwe: Geology, v. 24, no. 9, pp. 823-826.

Galarza Toro, M. A., 2002, Geocronologia e geoquímica isotópica dos depósitos de Cu-Au Igarapé Bahia e Gameleira, Província mineral dos Carajás (PA), Brasil: Unpublished Ph.D. thesis, Instituto de Geociências, Universidade do Pará, 213 pp.

Guimarães, I.G., 1987, Petrologia das formações ferríferas da área do Salobo 3A, Província Mineral dos Carajás - Estado do Pará: Unpublished MSc thesis, Instituto de Geociências, Universidade São Paulo, 139pp.

Gomes, C. B., Cordani, U. G., and Basei, M. A. S., 1975, Radiometric ages from Serra dos Carajás area, northern Brazil: Geological Society America Bulletin., v.86, pp.938-942.

Hitzmann, M. W., Oreskas, N., and Einandi, M. T., 1992, Geological characteristics and tectonic setting of Proterozoic iron-oxide (Cu-U-Au-REE) deposits: Precambrian Research, v.58, pp. 241-287.

Hunh, S. R. B., and Nascimento, J. A. S., 1997, São os depósitos cupríferos de Carajás do tipo Cu-Au-ETR? *In*: Costa, M.L. and Angelica, R.S., eds., Contribuições à Geologia da Amazônia, BelÉm, SBG, pp. 143-160.

Lindenmayer, Z. G., 1990, Salobo Sequence, Carajás, Brazil: Geology, geochemistry and metamorphism: Unpublished Ph.D. thesis, University of Western Ontario, Ontario, 405pp.

Lindenmayer, Z. G., 1999, Ore genesis at the Salobo cooper deposit, Serra dos Carajás. *in*: Silva, M. da G. and Misi, A., eds., Base Metal Deposits of Brazil, Belo Horizonte, MME/CPRM/DNPM, pp. 33-43.

Lindenmayer, Z. G., Fife, W. S., and Bocalon, V. L. S., 1994, Nota preliminar sobre as intrusões granitóides do depósito de cobre do Salobo, Carajás: Acta Geológica Leopoldinensis, v. 40, pp. 153-182.

Ludwig, K. R., 1998, Isoplot/Ex. Berkeley Geochronological Center. Special Publication 1, 41pp.

Macambira, M. J. B., Lafon, J. M., 1995, Geocronologia da província mineral de Carajás: Síntese dos dados e novos desafios: Boletim do Museo Paraense Emílio Goeldi, Série Ciências da Terra, v. 7, pp. 263-288.

Machado, N., Lindenmayer, Z., Krogh, T. E., and Lindenmayer, D., 1991, U-Pb geochronology of Archean magmatism and basement reactivation in the Carajás área, Amazon Shield, Brazil: Precambrian Research, v. 49, pp. 329-354.

Montalvão, R. M. G., Tassinari, C. C. G., and Bezerra, P. E. L, 1984, Geocronologia dos granitóides e gnaisses das regiões do Rio Maria, Fazenda Mata Geral e Rio Itacaiúnas, Sul do Pará (Distrito Carajás-Cumaru): Actas do XXXIII Congresso Brasileiro de Geologia, Rio de Janeiro, SBG, v. 6, pp. 2757-2766.

Mougeot, R., Respaut, J. P., Briqueu, L., Ledru, P., Milesi, J. P., Lerouge, C., Marcoux, E., Huhn, S. B., and Macambira, M. J. B., 1996, Isotope geochemistry constrains for Cu, Au mineralizations and evolutions of the Carajás Province (Pará, Brazil): Actas do XXXIX Congresso Brasileiro de Geologia, Salvador, SBG, v. 7, pp. 318-320.

NUCLEBRÁS (1985) Relatório do Projeto Itacaiúnas—parte texto. Relatório interno. Rio de Janeiro. 130pp.

Olszewski, W. J., Wirth, K. R., Gibbs, A. K., and Gaudette, H. E., 1989, The age, origin and tectonics of the Grão Pará Group and associated rocks, Serra dos Carajás, Brazil. Archean continental volcanism and rifting: Precambrian Research, v. 42, pp. 229-254.

Pinheiro, R. V. L., 1997, Reactivation history of the Carajás and Cinzento strike-slip systems, Amazon, Brazil: Unpublished Ph.D. thesis, University of Durham, England, 407pp.

Pinheiro, R. V. L., and Holdsworth, R. E., 1997, Reactivation of Archean strike-slip fault systems, Amazon region, Brazil: Journal of Geological Society of London, v. 154, pp. 99-103.

Réquia, K. M. C., Xavier, R. P., and Figueiredo, B., 1997, Evolução paragenética, textural e das fases fluidas no depósito polimetálico de Salobo, Provincia Mineral de Carajás, Pará: Boletim do Museo Paraense Emílio Goeldi, Série Ciências da Terra, v. 7, pp. 27-39.

Siqueira, J. B., 1990, Organização litoestrutural do dúplex Salobo-Mirim, Serra dos Carajás, PA: Unpublished MSc. thesis, Instituto de Geociências, Universidade do Pará, Belém, 125pp.

Siqueira, J. B., 1996, Aspectos litoestruturais e mineralizações do Depósito do Salobo 3A (Serra dos Carajás/PA): Unpublished Ph.D. thesis, Instituto de Geociências, Universidade do Pará, Belém, 156pp.

Tassinari, C. C. G., Hirata, W. K., and Kawashita, K., 1982, Geologic evolution of the Serra dos Carajás, Pará, Brazil: Revista Brasileira de Geociências, v. 12, nos. 1-3, pp. 263-267.

Tassinari, C. C. G., and Macambira, M. J. B., 1999, Geochronological Provinces of the Amazonian Craton: Episodes, v. 22, no. 3, pp. 174-182

Colombo Celso Gaeta Tassinari *is a full professor of isotope geochemistry at Institute of Geoscience of University of São Paulo and head of Geochronological Research Center of the same University. He works on isotope geology applied to crustal evolution and metallogenesis. He was joint leader of two IGCP Projects: 204 "Geological Evolutions of the Amazonian Craton" and 342 "Isotopes in South American Ores".*

Marly Babinski *graduated in geology in 1984. She got her Master's (1988) and Ph. D. (1993) degrees at the University of São Paulo (USP). She is Assistant Professor at the Institute of Geosciences and Vice-director of the Geochonology Research Center at USP. She works on geochronology of sedimentary rocks and associated mineralizations.*